C-Myc–Independent Restoration of Multiple Phenotypes by Two C-Myc Target Genes with Overlapping Functions

Krisiti Rothermund,[1] Kenneth Rogulski,[1] Elaine Fernandes,[1] Amy Whiting,[4] John Sedivy,[4] Lixia Pu,[1] and Edward V. Prochownik[1,2,3]

[1]Section of Hematology/Oncology, Children's Hospital of Pittsburgh; [2]University of Pittsburgh Cancer Institute; [3]Department of Molecular Genetics and Biochemistry, University of Pittsburgh Medical Center, Pittsburgh, Pennsylvania; and [4]Department of Molecular Biology, Brown University, Providence, Rhode Island

Abstract

***C-MYC*, a transforming oncogene that is frequently overexpressed in many human cancers, regulates a variety of normal functions including cell cycle progression, apoptosis, and maintenance of cell size, morphology, and genomic integrity. Many target genes are modulated by c-Myc, and some can recapitulate a limited number of the above functions. Because most of these have been assessed in cells which also express endogenous c-Myc, however, it is not clear to what extent its proper regulation is also required. We show here that, in c-Myc nullizygous cells, two direct target genes, *MT-MC1* and *HMG-I*, could each recapitulate multiple c-Myc phenotypes. Although these differ somewhat for the two genes, substantial overlap and cooperativity exist. The enforced expression of these two genes was also associated with the differential deregulation of some previously described c-Myc target genes, indicating the presence of a complex molecular circuitry. These observations argue that, despite the great diversity of gene regulation by c-Myc, many, although not all, of its functions can be phenocopied by a small subset of key downstream target genes. The approach described here should permit the identification of other target genes capable of further c-Myc–independent complementation.** (Cancer Res 2005; 65(6): 2097-107)

Introduction

Members of the Myc oncoprotein family are frequently overexpressed in human cancers (1). All of these, including c-Myc, the most commonly involved member, are basic helix-loop-helix leucine zipper transcription factors, which regulate the transcription of numerous genes involved in various functions relevant to transformation (2, 3). Furthermore, the control of these genes by c-Myc can be either positive or negative (4–12). The importance of c-Myc as a general transcription factor is underscored by recent studies suggesting that as much as 10% to 15% of the expressed genome may be at least partially c-Myc-responsive (9, 13). c-Myc overexpressing cells often display morphologic abnormalities, cell size differences, aberrant cell cycle control, loss of growth factor responsiveness, inability to differentiate, enhanced sensitivity to proapoptotic stimuli, and genomic instability (14–27).

Although the complete catalog of c-Myc target genes has not been studied in detail, some genes, when individually overexpressed, can recapitulate a limited number of the c-Myc phenotypes described above (23, 28–38). The restricted functions of these target gene products, however, has supported the idea that multiple, functionally redundant genes, acting in concert, are necessary to impart the complex c-Myc phenotype. A major challenge is to determine which of these genes comprise the minimal functional subset and whether it is unique or interchangeable with other such subsets. Another challenge is to determine whether the restricted c-Myc-like properties imparted by individual targets require assistance in the form of concurrent expression of endogenous c-Myc and/or of its other downstream targets.

The direct c-Myc target gene, *MT-MC1*, encodes a nuclear protein with homology to certain DNA helicases (38). Unlike the limited functions of other c-Myc target genes described above, overexpression of MT-MC1 leads to morphologic alterations, enhanced apoptosis, promotion of cell cycle progression, inhibition of differentiation, induction of genomic instability, transformation, and the regulation of some c-Myc target genes. Thus, MT-MC1 is unique among c-Myc targets by virtue of its ability to recapitulate a global c-Myc phenotype.

Another direct c-Myc target gene, *HMG-I/Y*, encodes two isoforms of the high-mobility group of chromatin modifying nuclear proteins (39–41). These proteins, HMG-I and HMG-Y, arise as a result of alternate mRNA splicing, differ by an 11 amino acid insertion in the former, and seem to possess identical functions (39). In addition to their role in chromatin maintenance, HMG-I/Y proteins also interact with and modify the activities of a number of transcription factors and may participate in DNA repair activities (reviewed in ref. 42). HMG-I/Y levels correlate with proliferation and their overexpression is associated with some experimental and naturally occurring tumor types, a number of which also overexpress c-Myc (43–48). Consistent with this association, HMG-I overexpression can lead to transformation both *in vitro* and *in vivo* (33, 49). Overall, however, HMG-I's c-Myc-like properties seem somewhat more restricted than those of MT-MC1.

The above functions of MT-MC1 and HMG-I suggest that they play important and perhaps central roles in orchestrating the complex c-Myc phenotype. However, because all of the cell types in which these proteins have been studied also express endogenous c-Myc, it remains unclear whether their effects are totally independent of c-Myc or require its concurrent expression and thus the proper regulation of additional downstream targets. The functional relatedness of MT-MC1 and HMG-I also remains undefined.

Knockout (KO) cells are a line of rat fibroblasts, which as a consequence of gene targeting, express neither endogenous c-Myc

Note: Supplementary data for this article are available at Cancer Research Online (http://cancerres.aacrjournals.org/).

Requests for reprints: Edward V. Prochownik, Section of Hematology/Oncology, Children's Hospital of Pittsburgh, Rangos Research Center, Room 2100, 3460 Fifth Avenue, Pittsburgh, PA 15213. Phone: 412-692-6797; Fax: 412-692-5228; E-mail: PROCEV@chp.edu.

nor other c-Myc family members (50, 51). Unlike other cells, in which inactivation of c-Myc results in the abrupt cessation of cell cycle progression and growth arrest (52), KO cells proliferate, albeit at a markedly reduced rate compared with the parental cell line from which they are derived (50). KO cells have thus been of considerable use in assessing both the functional consequences of c-Myc loss and in determining whether and to what extent other genes can substitute for c-Myc (29, 31, 35, 51, 53).

Because MT-MC1 and HMG-I can mimic some of the above-described c-Myc phenotypes, we have now asked whether they can also do so in KO cells and whether their effects are unique, complementary, or additive. As presented below, our results show that many, although not all, of the phenotypes imparted by MT-MC1 and HMG-I are indeed mimicked in KO cells and are therefore c-Myc–independent. Furthermore, whereas some of the phenotypes imparted by each gene are distinct, they also display functional redundancy and cooperation. Thus, despite the complexity of both the c-Myc genotype and phenotype, significant c-Myc–independent recapitulation of the latter can be achieved with only two of its downstream targets.

Materials and Methods

Cell Lines. The rat fibroblast cell lines TGR1 and its "knockout" derivative (HO16.4c, or "KO" cells) have been previously described (50). The latter were derived by homologous recombination with a c-Myc targeting vector, and express neither endogenous c-Myc nor other c-Myc family members such as N-Myc and L-Myc. Propagation and transfection of the amphotropic Phoenix-A retroviral packaging cell line have been previously described (51). All cell lines were routinely maintained in standard growth medium consisting of DMEM supplemented with 10% FCS, glutamine, and penicillin plus streptomycin as described (all from Life Technologies, Grand Island, NY; refs. 38, 51). KO cells were also periodically cultured in the presence of 250 μg/mL G-418 (Life Technologies). Growth curves were done in 12-well tissue culture plates. Each cell line was plated in standard growth medium at 8×10^3 cells per well. At various times thereafter, triplicate wells were trypsinized and the average number of viable cells per well was determined by trypan blue exclusion using a hemacytometer. Soft agar colony assays were done as previously described (38), with all colonies being enumerated after 10 to 12 days and plating at 4×10^3 cells/60 mm dish. When measuring colony formation by slowly growing cells, cultures were fed weekly and evaluated after 4 weeks.

Retroviral Constructs, Packaging, and Infection. Full-length murine MT-MC1 was amplified from the pSVLneoMT-MT-MC1 vector (38) by PCR using primers containing engineered *Xho*I restriction sites. Following digestion with *Xho*I, the product was isolated from a 2% agarose gel and ligated into the unique *Xho*I site of the bicistronic pBabe-MN-IRES-GFP vector (51), which had been previously modified by inserting a c-Myc epitope tag containing an optimized Kozak consensus site. The resultant vector thus contained the MT-MC1 coding region fused in-frame at its 5′-end with the c-Myc epitope tag. The correct orientation and reading frame of the insert was confirmed by DNA sequencing. The construct, or the starting parental vector, was then transiently expressed in Phoenix-A packaging cells following transfection with LipofectAMINE (Life Technologies).

The human HMG-I coding region was also amplified by PCR using primers containing *Xho*I sites. After isolation and *Xho*I digestion, the cDNA fragment was cloned into a modified form of the above-described retroviral vector in which the enhanced green fluorescent protein (GFP) coding sequence had been replaced with that of dsRed (BD Biosciences/Clontech, Inc., Palo Alto, CA) and in which the c-Myc epitope tag had been fused to the 3′-end of the HMG-I cDNA. Phoenix-A transfection efficiencies with both retroviral vectors, as well as their starting parental vectors, routinely exceeded 50% and were monitored by observing GFP-positive or dsRed-positive cells at 48 hours. Viral supernatants were harvested between 48 and 72 hours, filtered, and used to infect KO cells in the presence of 8 μg/mL Polybrene (Sigma, St Louis, MO) for 24 hours. KO transduction efficiencies were generally 20% to 40% based on GFP or dsRed positivity of the recipient cells 72 hours post-infection. Cells were then sorted and analyzed with a Becton Dickinson FACSVantage SE flow cytometer equipped with the FACSDiVa Option and CellQuest software. The cytometer was equipped with an INNOVA Enterprise Laser (Coherent, Inc., Santa Clara, CA). Cells were excited at a wavelength of 488 nm. GFP signals were collected on the FL1 (FITC) detector with a 530/30 bandpass filter and dsRed signals were collected on the FL2 (PE) detector with a 585/42 filter. Sorting gates were first drawn around FSC and SSC populations to eliminate obvious nonviable cells and debris. A subsequent gate was set on FL1- or FL2-positive cells. A post-sort analysis was done to determine the purity of sorted cells, which, in all cases, exceeded 95%. This was also confirmed by direct visual inspection of the sorted cells using fluorescence microscopy. The resulting cell lines were designated KO-MT-MC1, KO-HMG-I, or KO-MT-MC1/HMG-I to denote single or double transductants, respectively. The latter cell line was derived by transduction of early passage KO-MT-MC1 cells with the HMG-I encoding retroviral vector. Cell lines arising from transduction with the individual parental enhanced GFP- or dsRed-encoding retroviral vectors were used as controls for KO-MT-MC1 and KO-MT-MC1/HMG-I cells, respectively, whereas a dual-transduced cell line was used as the control for KO-MT-MC1/HMG-I cells. In all cases, these control lines are referred to as "KO-vector" cells; their behaviors were identical to one another and were indistinguishable from nontransduced KO cells (data not shown).

Filamentous Actin Staining. Cells were cultured in 8-well chambers (Lab Tek Chamber Slides, Nalge-Nunc, Naperville, IL) at 37°C for 24 hours, washed thrice with PBS, and fixed with 3.7% formaldehyde in PBS at room temperature for 10 minutes. Slides were then washed three additional times with PBS. Cells were permeabilized with imidazole lysis buffer [10 mmol/L imidazole (pH 7.15), 40 mmol/L KCl, 10 mmol/L EDTA, 0.2% Triton X-100] for 15 minutes and then stained in the same buffer containing 0.5% bovine serum albumin and 3 units/mL of Oregon green phalloidin 514 (Molecular Probes, Eugene, OR) for 35 minutes in the dark at room temperature. After washing thrice with PBS, cells were counterstained at room temperature for 5 minutes with 100 mmol/L 4′,6-diamidino-2-phenylindole in the dark. Following an additional wash in PBS, slides were treated with antifade reagent (Molecular Probes) before applying coverslips. Cells were observed with a Nikon Eclipse E800 fluorescent microscope equipped with a FITC filter. Stained nuclei were visualized using a 4′,6-diamidino-2-phenylindole filter. Superimposed images (×100) were acquired using the Magnafire 2.1 program.

Cell Size Determinations. Adherent cells in mid-log phase growth were washed twice with PBS and trypsinized. An aliquot was stained with propidium iodide and analyzed by flow cytometry to ensure that each cell line contained equal populations of cells in G_0/G_1, S, and G_2-M phases. The remaining cells were resuspended in cell culture medium in the presence of trypan blue. The diameters of at least 2,500 individual cells per sample were determined on at least three separate occasions with a Vi-Cell Viability Analyzer (model 1.0, Becton-Coulter, Inc., Miami, FL) and the results were pooled. A video imaging system was used to distinguish viable and dead cells, with only the former being included in the final total. In all cases, viability exceeded 95%.

Statistical analysis used the software package SPSS (version 11.5, SPSS, Inc. Chicago, IL). ANOVA and Kruskal-Wallace procedures were used for comparisons among the various cell lines. The Tukey HSD procedure was used for *post hoc* pairwise comparisons between pairs of groups.

Protein and RNA Analyses. The expression of myc epitope-tagged MT-MC1 and HMG-I in KO cells was routinely monitored by Western analyses of total cell lysates as previously described (38). Briefly, 50 μg of total protein was resolved on 12% polyacrylamide-SDS gels and transferred to polyvinylidene difluoride membranes (Millipore, Bedford, MA). After blocking with 5% dried milk in PBS + 2.5% Tween 20, the blot was incubated with a 1:500 dilution of the 9E10 anti-c-Myc monoclonal antibody (#sc-40, Santa Cruz Biotechnology, Santa Cruz, CA). As a control for protein loading, blots were also probed with an anti-β-tubulin

monoclonal antibody (#05-661, Upstate Biotechnology, Lake Placid, NY). After extensive washing in PBS + 2.5% Tween 20 blots were incubated with a 1:2,500 dilution of horseradish peroxidase-conjugated goat anti-mouse IgG (#sc-2005, Santa Cruz), washed in PBS + 2.5% Tween 20, and developed using a "Western Lightning" chemiluminescence kit (Perkin-Elmer Life Sciences, Boston, MA) according to the directions of the supplier.

Northern blots (5 μg total RNA/lane) were prepared as previously described (22, 38). Probes consisted of ^{32}P-labeled cDNAs, or synthetic oligonucleotides, 38 to 40 nucleotides in length. Conditions for hybridization in Ultra Hyb (Ambion, Austin, TX) and post-hybridization washings have been previously described (23, 38).

For quantitative real-time PCR analyses, a Quantitect SYBR Green kit (Qiagen, Inc., Valencia, CA) was used. Total RNA (50 ng) from each cell line was reverse-transcribed and the product subsequently amplified in a total volume of 20 μL in the presence of 1 μmol/L concentrations of each PCR primer (ca. 100 ng per reaction). Each primer set was synthesized so as to span an intron in the corresponding target gene. A list of PCR primers is included in Supplementary Table 1. The initial real-time syntheses were done for 20 minutes at 50°C. PCR reactions were done in a LightCycler 2.0 apparatus (Roche Diagnostics, Indianapolis, IN) using a 15-minute activation step at 95°C. A total of 40 cycles of PCR were then carried out using a 15-second denaturation step at 94°C, 20 seconds of annealing at 55°C, and 30 seconds of extension at 72°C. All reactions were done a minimum of three times. Relative quantifications comparing the levels of each target RNA with that of the glyceraldehyde-3-phosphate dehydrogenase reference were done using Lightcycler quantification software version 4.0. An amplification efficiency of 2 was used in the analysis.

Results

MT-MC1 and HMG-I Alter the Morphology of Knockout Cells. In order to study the c-Myc–independent consequences of MT-MC1 and/or HMG-I overexpression, we infected KO cells with retroviruses encoding each of these epitope-tagged proteins. In the first case, the bicistronic retroviral vector also encoded enhanced GFP under the control of an internal ribosome entry site, whereas in the second case, the vector encoded dsRed variant of *Discosoma* sp. red fluorescent protein (BD Biosciences/Clontech). The differences in emission/excitation spectra of the two fluorescent proteins allowed for pure, pooled populations of sequentially transduced cells to be readily isolated by fluorescence-activated cell sorting. As controls, KO cells were also infected singly or sequentially with the empty parental retroviruses and isolated in the same way. Transduced cell lines were then examined for the expression of MT-MC1 and HMG-I by Western blotting. As seen in Fig. 1*A*, these cells (hereafter designated KO-MT-MC1, KO-HMG-I, and KO-MT-MC1/HMG-I cells) expressed high levels of both proteins. As expected, KO-vector cells expressed neither protein (Fig. 1*A*).[5]

Northern analyses of the above cell lines showed that endogenous MT-MC1 and HMG-I transcripts were expressed at low to undetectable levels relative to those present in retrovirally transduced cells (Fig. 1*B*). However, the levels of these latter transcripts were comparable to the endogenous levels seen in 32D myeloid cells, particularly those with deregulated c-Myc expression. Thus, the retroviral transduction of both MT-MC1 and HMG-I in KO cells resulted in levels of expression attainable in other cell types.

Compared with parental TGR1 cells, KO cells possess a flattened, "cuboidal" morphology and occupy a larger surface area. This phenotype can be rescued by the overexpression of c-Myc or other members of the Myc family (50, 51). In order to determine whether this phenotype could also be rescued by MT-MC1 and HMG-I in a c-Myc–independent manner, we compared the morphologies of the above cell lines, as well as that of the TGR1 parental cell line using Oregon green-conjugated phalloidin. This cyclic peptide derivative of the mushroom *Amanita phalloides* selectively binds to filamentous actin (F-actin) to reveal its typical cable-like pattern in fibroblasts (54). In TGR1 cultures, F-actin cables were invariably oriented parallel to the main axes of the highly elongated cells (Fig. 1*C*). In addition, the pattern was somewhat indistinct, most likely owing to the greater relative thickness of the cells. In three separate experiments, virtually all the cells showed this typical fibroblastoid pattern. In contrast, the F-actin patterns of nearly all KO and KO-vector cells, were distinctly different, with a much better defined cable network that was longer, seemingly thicker, and more randomly arrayed. This staining also clearly emphasized the larger surface area of the cells. Reconstitution with c-Myc resulted in a correction of the morphologic defect in 42% of the cells.

We next asked whether the expression of MT-MC1 and HMG-I could alter the morphology of KO cells. In the first case, MT-MC1 promoted the reversion of 22% of KO cells; the morphology of these was virtually indistinguishable from that of TGR1 and KO-c-Myc cells. HMG-I also promoted morphologic changes in virtually all cells. However, the appearance of these cells was distinctly different, as they retained the overall cuboidal appearance of KO cells, whereas at the same time appearing less spread out and showing a less well-defined F-actin cable pattern reminiscent of TGR1 cells. A greater amount of intense F-actin staining was also observed at the edges of pseudopods.

Finally, 61% of KO-MT-MC1/HMG-I showed morphologies characteristic of each of the previously described cell lines expressing the individual proteins. From these results, we conclude that MT-MC1 and HMG-I each alters the structure of KO cells in distinct ways and that these changes are c-Myc–independent.

Correction of the Growth Defect of Knockout Cells by MT-MC1 and HMG-I. KO cells divide significantly more slowly than either parental TGR1 cells or TGR1 cells with a single c-Myc allele (50). We and others have previously shown that c-Myc and other members of the Myc family can rescue this growth defect (50, 51). In order to determine whether MT-MC1 and HMG-I could affect the growth rate of KO cells, we examined this property in each of the transduced cell lines within 2 weeks of their derivation. As seen in Fig. 2*A*, KO-MT-MC1 cells initially grew at the same slow rate as KO and KO-vector cells (doubling times, ca. 50-60 hours). However, upon longer *in vitro* propagation (ca. 10-12 weeks), these cells reproducibly acquired a markedly accelerated growth rate (Fig.2*B*). In contrast, even the earliest passage KO-HMG-I and KO-MT-MC1/HMG-I cells showed rapid growth rates (doubling times, ca. 14-16 hours; Fig. 2*A*). This was seen in several independent experiments, thus indicating that it was a general and direct consequence of the HMG-I's ectopic expression. Furthermore, unlike KO-c-Myc cells, which underwent massive apoptosis upon reaching saturation density, KO-HMG-I and KO-MT-MC1/HMG-I cells continued to proliferate, ultimately attaining a 6- to 8-fold higher saturation density, and remaining viable without any evidence of apoptosis even following serum deprivation (Fig. 2*C* and data not shown). Thus, MT-MC1 and HMG-I each rescues the growth defect of KO cells, but does so in distinct ways, with HMG-I's effect being immediate and dominant over that of MT-MC1.

[5] Unpublished observations.

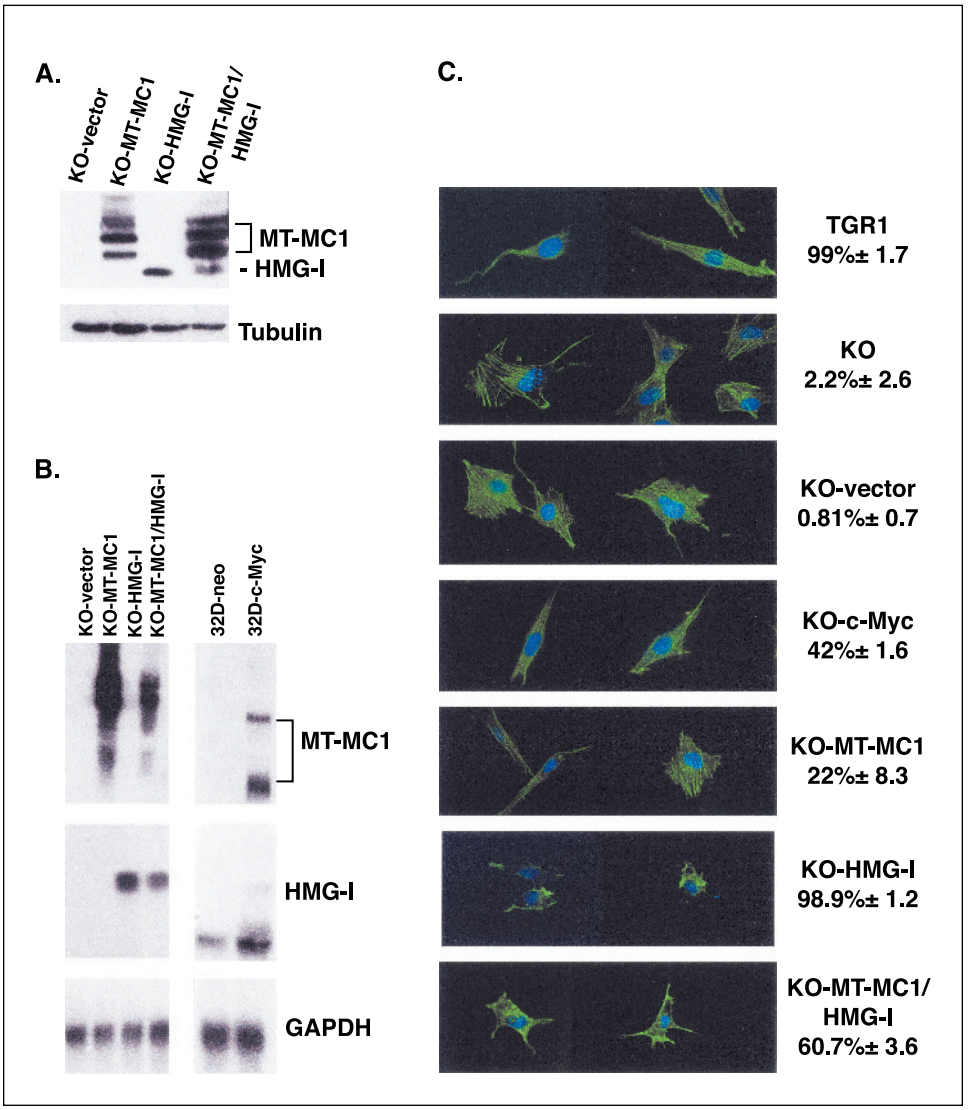

Figure 1. Expression of MT-MC1 and HMG-I, and F-actin staining patterns in various fibroblast lines. *A,* expression of MT-MC1 and HMG-I. Western blots from the indicated cell lines were used to detect Myc-epitope-tagged MT-MC1 and HMG-I; *bottom,* the same blot probed for tubulin expression as a control for protein loading; *B,* comparisons of MT-MC1 and HMG-I transcript levels. Northern analyses were done on the indicated cell lines. c-Myc-overexpressing 32D murine myeloid cells (32D-c-Myc cells) or control 32D (32D-neo cells; ref. 38) were included as controls to show the c-Myc-mediated induction of endogenous MT-MC1 and HMG-I. Note that the former consists of two transcripts, which arise by alternate polyadenylation site selection (38). Glyceraldehyde-3-phosphate dehydrogenase was included as a control for RNA loading. The larger MT-MC1 and HMG-I transcripts in the fibroblast lines are due to their being encoded by the retroviral genome; *C,* F-actin staining patterns. Each of the indicated cell lines was stained with Oregon green-conjugated phalloidin. KO-c-Myc cells were derived by transduction with the same enhanced GFP-encoding bicistronic retroviral vector and have been previously described (51). TGR1 cells are the parental c-Myc+/+ fibroblasts from which the KO line was derived (50). Numbers indicate the percent of cells from at least three separate experiments (± 1 SE) demonstrating morphologies distinct from that of KO cells. In each case, percentages were calculated from 100 to 200 cells per group.

Both TGR1 and KO cells are quite resistant to apoptosis following serum deprivation. In contrast, KO-c-Myc cells are highly prone to apoptosis even when maintained in serum-containing medium at high density (ref. 51 and Fig. 2*C*). Interestingly, neither MT-MC1 nor HMG-I altered the intrinsic resistance of KO cells to serum deprivation (data not shown). Thus, despite the effects of these two c-Myc target genes on cell growth, they exerted no significant effect on survival under conditions in which c-Myc itself is highly proapoptotic.

Differential Effects of MT-MC1 and HMG-I on Genomic Integrity. c-Myc overexpressing cells often show genomic instability. Depending on the cell type, this can be manifested by an increase in chromosomal number, by frequent chromosomal breaks and translocations, by the amplification of certain genomic loci, or by the introduction of point mutations resulting from high levels of oxidative DNA damage (20, 22–24, 55, 56). We and others have shown that tetraploidy can be induced in c-Myc-overexpressing diploid cells if they are exposed to mitotic spindle poisons, if the p53 tumor suppressor is inactivated, or if the G_2-M mitotic cyclin, cyclin B1, is deregulated (20, 22, 23). The ability of c-Myc to confer this property is time-dependent, suggesting that at least some aspects of the c-Myc-mediated loss of genomic integrity are indirect and stochastic in nature (22, 23, 57). More recently, we have shown that MT-MC1 overexpression also leads to tetraploidy. As in the case of c-Myc, this occurs following exposure to mitotic spindle poisons but can also arise spontaneously during the course of *in vitro* passage (ref. 38 and data not shown).

In order to investigate the consequences of MT-MC1 and HMG-I overexpression on genomic integrity, we periodically assessed the DNA content of the various KO cell lines. As seen in Fig. 3*A*, KO and KO-vector cells remained diploid over the course of the study, as did KO-HMG-I cells. In contrast, although early passage KO-MT-MC1 cells were initially diploid, they became progressively more tetraploid with continued propagation (Fig. 3*A* and *B*). Depending upon the experiment, this first became evident 4 to 8 weeks after the derivation of the cell line. Interestingly, no evidence of tetraploidy was seen in KO-MT-MC1/HMG-I cells even when propagated for >6 months. We conclude that only MT-MC1 has the ability to noticeably affect genomic stability and that it does so in a c-Myc–independent manner. Like c-Myc, MT-MC1 seems to modulate chromosomal number indirectly, as evidenced by the fact that tetraploidy occurs only after prolonged *in vitro* passage.

The delayed effect of MT-MC1 on growth could have resulted from the expansion of a single KO clone or small number of clones as a consequence of retroviral activation of a growth-enhancing gene or the inactivation of a growth suppressor. Arguing against this was the observation that enhanced KO-vector cell proliferation was never observed and that the delayed onset of KO-MT-MC1 rapid growth was seen on several independent occasions (data not shown). However, to examine this directly, we asked whether late passage KO-MT-MC1 cells might show evidence of unique retroviral integration sites. Southern blots from both early and late passage KO-MT-MC1 cells using the GFP coding region as a probe produced a diffuse signal, indicative of multiple retroviral insertion sites within each cell population (Fig. 3*C* and *D*). In contrast, digestion of DNA with enzymes whose recognition sites flanked the IRES-GFP cassette in the retroviral genome produced a single autoradiographic band (Fig. 3*E*). We conclude that MT-MC1's ability to accelerate growth did not arise from a proliferative advantage conferred upon a small subset of retrovirally transduced clones.

MT-MC1 and HMG-I Affect Cell Size in Opposite Ways. Another feature of c-Myc is its ability to promote an increase in the size and mass of certain cell types (18, 19, 27). This may relate to c-Myc's ability to up-regulate the expression of genes involved in ribosomal biogenesis and metabolism and to its induction of RNA polymerase III-mediated transcription (58). To determine whether MT-MC1 and HMG-I could exert a similar effect, we compared the sizes of the various KO cell lines. Cells were harvested in mid-log phase growth and their cell cycle profiles were determined by propidium iodide staining prior to measuring their sizes (data not shown). Each cell line contained comparable G_0/G_1, S, and G_2-M populations and were fully diploid, thus eliminating the possibility that any observed size differences could be due to unequal cell cycle distribution profiles. When analyzed in this way, KO and KO-vector cells

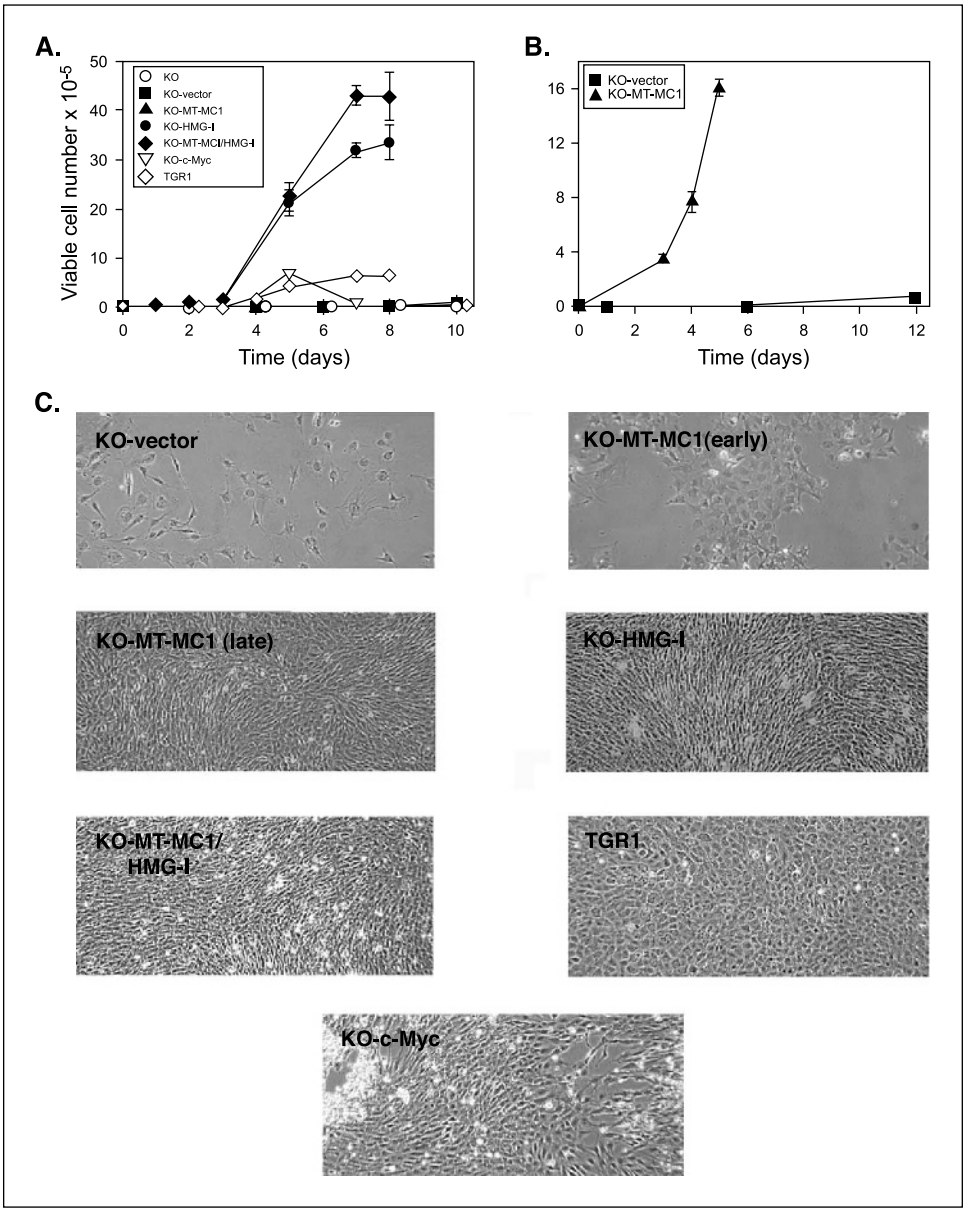

Figure 2. Growth rates of KO cell lines. *A,* growth rates of the indicated cell lines were compared ~2 weeks after their derivation. The doubling times of the KO cell line and all three KO-vector cell lines was estimated to be 50 to 60 hours, whereas TGR1 cells had a doubling time of ca. 20 hours as previously described (50, 51). Early passage KO-MT-MC1 cells had a doubling time similar to that of KO and KO-vector cells, whereas KO-HMG-I, KO-MT-MC1/HMG-I, and KO-c-Myc cells grew significantly faster (doubling time, ca. 14-18.5 hours). Although difficult to appreciate due to the linear nature of the abscissa, all of the cell lines except KO, KO-vector, and KO-MT-MC1 increased to between 8×10^4 and 1.6×10^5 from days 1 to 3, and continued to increase exponentially until reaching saturation density; *B,* growth rates of KO-MT-MC1 and KO-vector cells were compared 12 weeks after their derivation. The doubling time of the former cell line was 22 to 24 hours. In all cases, the results show the average number of cells determined in triplicate experiments $\pm$ 1 SE; *C,* phase-contrast micrographs of cell monolayers taken 6 days after plating equivalent numbers of cells. Note that significant numbers of KO-c-Myc cells are undergoing apoptosis even before reaching complete confluence.

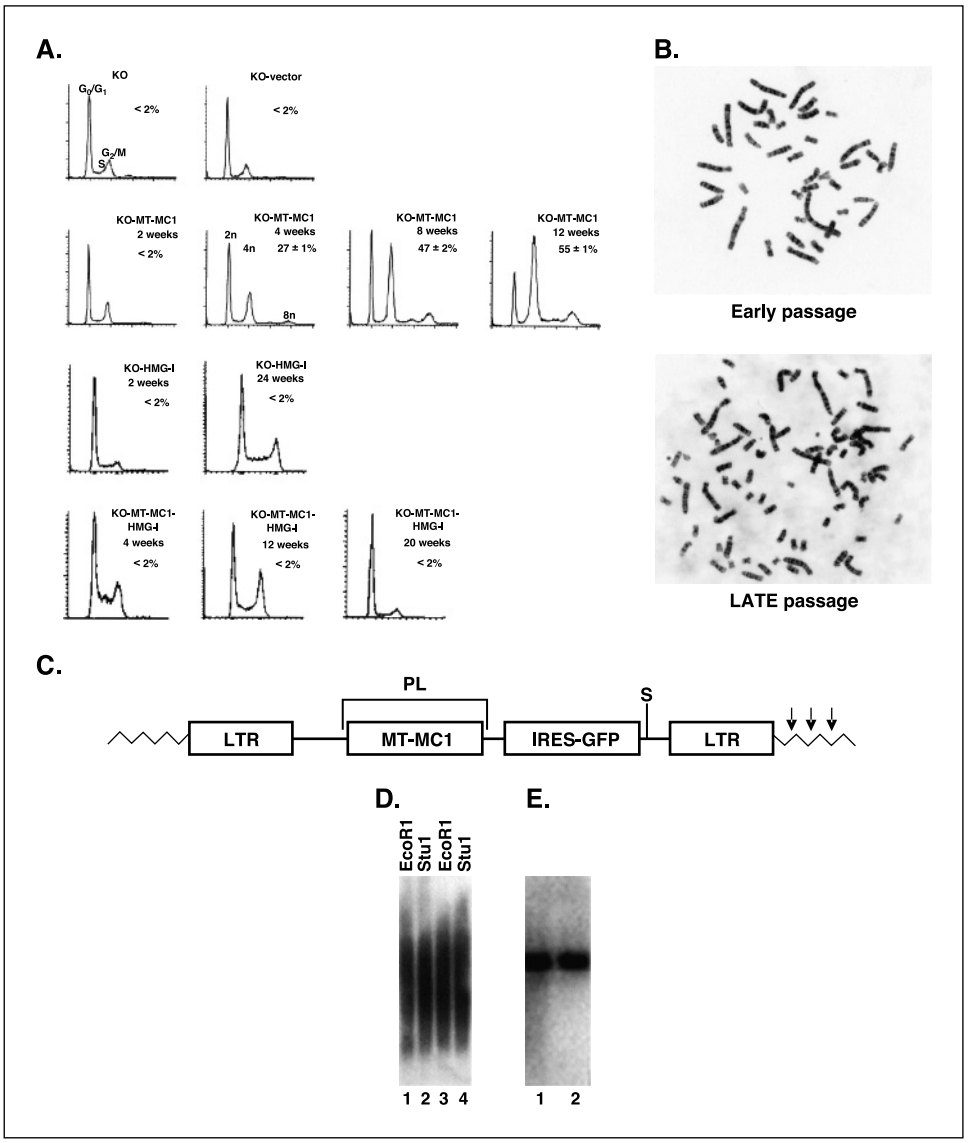

Figure 3. Nuclear DNA content and karyotypes of KO cell lines. *A,* nuclear DNA content of the indicated cell lines was evaluated by flow cytometry of propidium iodide-stained nuclei at the indicated times after derivation. Note the progressive accumulation of tetraploid KO-MT-MC1 cells. Numbers indicate the percentage of tetraploid cells; *B*, typical karyotypes of early passage (ca. 2 weeks) and late passage (ca. 12 weeks) KO-MT-MC1 cells. At least 50 cells of each passage were examined. No evidence of tetraploidy was seen in early passage cells, whereas two-thirds of the karyotypes of late passage cells were tetraploid, in good agreement with the cell cycle analyses shown in (A); *C*, structure of the integrated pBabe-MN-IRES-GFP retroviral vector containing epitope tagged MT-MC1 (not to scale). *Wavy lines*, flanking genomic DNA; PL, polylinker of the vector, which contains restriction sites for *Bam*HI, *Eco*RI, *Stu*I, and *Xho*I immediately upstream of the MT-MC1 coding region and for *Not*I/*Eag*I immediately downstream; *S,* a unique *Sal*I site immediately adjacent to the IRES-GFP cassette; *arrows,* genomic restriction sites in different clones at variable distances from the point of viral integration; *D,* Southern blots done with total genomic DNAs extracted from early (*lanes 1* and *2*) and late passage (*lanes 3* and *4*) KO-MT-MC1 cells. Ten micrograms of genomic DNA from each cell line was digested with the indicated restriction enzymes. After transfer, the blot was probed with a coding region probe for GFP; *E,* southern blots of the same early (*lane 1*) and late (*lane 2*) passage KO-MT-MC1 genomic DNAs digested with *Eag*I and *Sal*I. Note the presence of a unique ca. 1.2-kb band.

were of comparable size, whereas both KO-c-Myc and early passage KO-MT-MC1 cells were significantly larger (Fig. 4). When the measured diameters of these cells were used to calculate their volumes (assuming a spherical shape), KO-MT-MC1 cells were ~15% larger than their KO-vector counterparts. In contrast to these findings, the average size of KO-HMG-I cells was actually somewhat smaller than that of KO or KO-vector cells. Interestingly, the combined expression of MT-MC1 and HMG-I cells resulted in a near normalization of cell size. Thus, both MT-MC1 and HMG-I/Y alter the size of KO cells in a c-Myc–independent manner, but do so in opposing ways.

Clonogenicity and Tumorigenicity of Knockout Cell Lines. Rat1a fibroblasts, which express endogenous c-Myc, can be transformed by either MT-MC1 or HMG-I. These cells show efficient clonogenic growth in soft agar and are tumorigenic in nude mice (33, 38). To determine whether these features were also c-Myc–independent, KO cell lines expressing each of the proteins were first plated in soft agar. As seen in Fig. 5*A* and *B*, late passage, but not early passage, KO-MT-MC1 cells formed anchorage-independent colonies, as did early passage KO-HMG-I and KO-MT-MC1/HMG-I cells. The cloning efficiency was lowest for KO-MT-MC1 cells, intermediate for KO-HMG-I cells, and highest for KO-MT-MC1/HMG-I cells. These differences were also mirrored in the sizes of the colonies: on average, those formed by KO-MT-MC1/HMG-I cells were significantly larger than were those formed by KO-MT-MC1 or KO-HMG-I cells (Fig. 5*B*). The relatively small size of colonies formed by other fibroblastoid cells expressing MT-MC1 has been previously noted (38).

The ability of each of the above cell lines to generate tumors *in vivo* mirrored their *in vitro* clonogenic ability. As seen in Fig. 5*C* and *D*, early passage KO-MT-MC1 were completely non-tumorigenic. In contrast, late passage KO-MT-MC1 cells as well as KO-HMG-I and KO-MT-MC1/HMG-I cells formed tumors in all animals, with the latter two lines showing a significantly faster rate of growth.

Regulation of c-Myc Target Genes by MT-MC1 and HMG-I. c-Myc–dependent regulation of numerous target genes in rat fibroblasts has been previously described (4, 5, 8, 11), as has the loss of this regulation in KO cells, and its correction by ectopically-expressed c-Myc (51, 53). The extent to which target gene

regulation by c-Myc occurs is dependent upon its affinity for genomic binding sites and its level of expression (9).

The above cell lines afforded the opportunity to determine whether functional complementation of c-Myc phenotypes by MT-MC1 and HMG-I was associated with altered expression of c-Myc target genes. To this end, we used a combination of Northern blotting and quantitative real-time PCR to examine the relative expression of a select subset of previously described c-Myc target genes (11). In the former case (Fig. 6*A*), the normal expression pattern of most of the genes tested in parental TGR1 cells was lost in KO-vector cells and restored in KO-c-Myc cells. A typical example was seen in the case of *gadd45*, which is a negative c-Myc target (59). In KO-vector cells, *gadd45* transcripts were increased relative to those in TGR1 cells, where they were barely detectable, whereas in KO-c-Myc cells, *gadd45* transcripts were strongly suppressed. Interestingly, neither MT-MC1 nor HMG-I repressed *gadd45* transcript levels when expressed individually, whereas their combined expression proved highly effective.

The serine hydroxymethyl transferase (*SHMT*) gene is a positive target for c-Myc (35). As expected, KO cells expressed lower levels of *SHMT* than did parental TGR1 cells. Ectopic expression of c-Myc, MT-MC1, or HMG-I individually resulted in a minimal or modest increase in *SHMT* transcript levels. In contrast, and in a manner reminiscent of the regulation described above for *gadd45*, MT-MC1 and HMG-I in combination proved highly effective at restoring *SHMT* transcript levels.

Two additional c-Myc targets, Apex and Prohibitin (11), showed similar patterns of expression; in both cases, reduced expression in KO cells was restored to normal or supra-normal levels only by HMG-I or c-Myc. This contrasted with another c-Myc target, ornithine decarboxylase, whose expression in KO cells was restored by MT-MC1 and c-Myc, but not by HMG-I.

c-Myc negatively regulates its own promoter (ref. 60 and references therein). Functional c-Myc transcripts are not expressed in KO cells due to the replacement of c-Myc coding sequences with a neo expression cassette (50). Neo transcripts thus serve as a surrogate marker of c-Myc promoter activity (51). As expected, neo transcripts were not detected in parental TGR1 cells but were expressed at high levels in KO cells, indicating that the c-Myc promoter was active. MT-MC1 did not affect the levels of neo transcripts, whereas both HMG-I, and c-Myc resulted in significant repression, as did the combined expression of MT-MC1 and HMG-I. Thus, both HMG-I and c-Myc were capable of down-regulating the c-Myc promoter.

Finally, we examined each of the cell lines for expression of N-Myc and L-Myc, which can substitute for c-Myc to restore a rapid growth phenotype to KO cells (51). Neither of these transcripts were detected.

Quantitative real-time PCR was next used to assess the regulation of several additional genes which were expressed at levels too low to be accurately quantified by Northern analyses (Fig. 6*B*). Some, but not all of these, were altered in KO cells

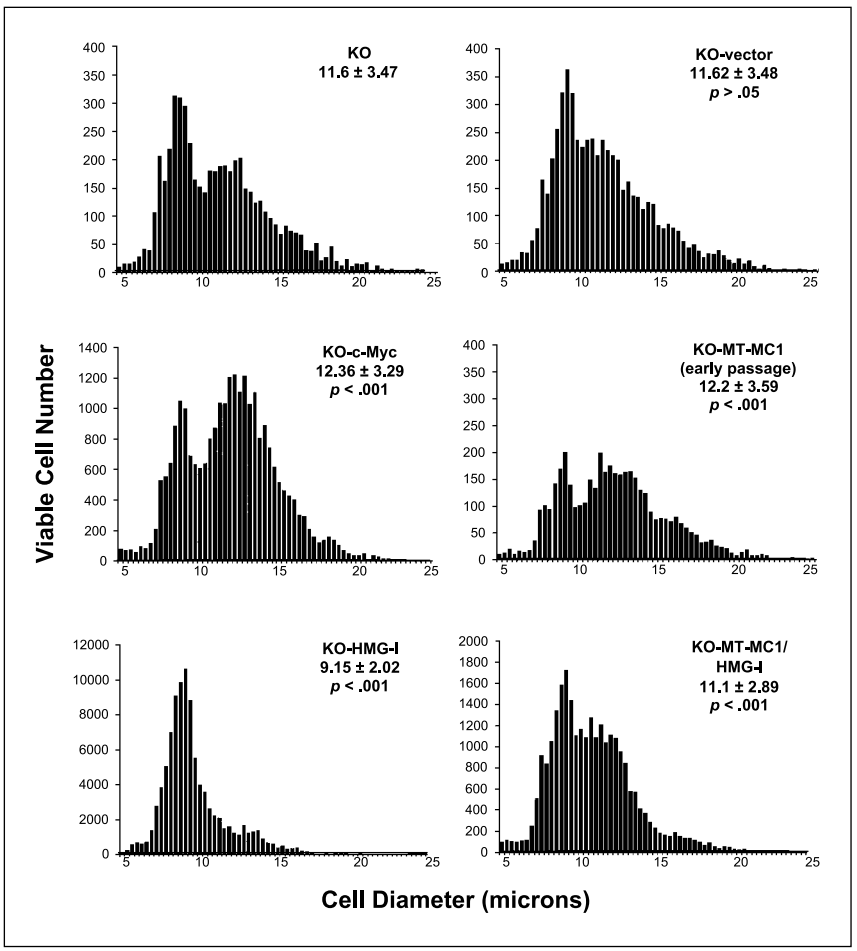

Figure 4. Cell size comparisons of KO cell lines. Each of the indicated cell lines was harvested in log-phase growth from cultures demonstrating ≥95% viability. Propidium iodide staining was done to confirm that all cell lines contained equal proportions of G_0/G_1, S, and G_2-M populations. Size determinations were done with a Vi-Cell Viability Analyzer (Beckman-Coulter). Numbers above the histograms indicate the average cell diameter ± 1 SE. *P* values are derived from comparison with the KO parental line using Student's two-tailed *t* test.

compared with TGR1 parental cells. For example, the transferrin receptor (a positive target for c-Myc) was expressed at a 3-fold lower level in KO versus TGR1 cells, whereas the reverse was true for Timp2 (a negative target). In other cases (for example, Nopp140 and Rcl), target transcripts were expressed at equivalent levels in TGR1 and KO cells. Such differential sensitivities to endogenous c-Myc have been previously noted (9, 11). Irrespective of these differences, however, all of the genes examined showed regulation by both ectopically expressed c-Myc and HMG-I but not by MT-MC1.

Although limited in scope, the above survey indicates that HMG-I and, to a lesser extent, MT-MC1, regulate some of the same c-Myc target genes.

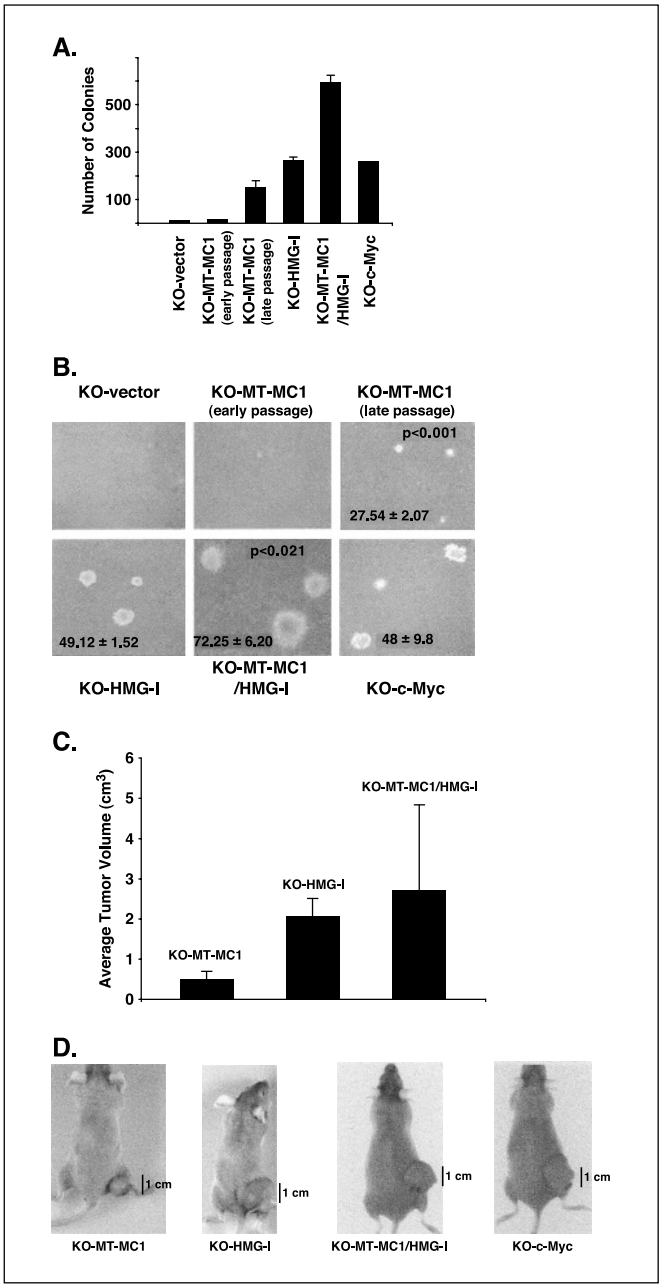

Figure 5. Differences in clonogenic and tumorigenic behaviors of KO cell lines. *A*, equivalent numbers of the indicated cell lines were plated in soft agar as previously described (38). After 12 to 14 days, the total number of colonies was determined from triplicate experiments; *B*, photomicrographs of typical agar colonies. The numbers shown at the bottom represent the average diameter of 100 to 200 randomly selected colonies ± 1 SE. *P* values shown at the top are based on the comparison of the size differences between late passage KO-MT-MC1 and KO-HMG-I colonies, and KO-HMG-I and KO-MT-MC1/HMG-I colonies; *C, in vivo* tumorigenicity of various KO cell lines. Cells of the indicated type (2×10^7) were inoculated s.c. into groups of five nude mice. Tumor growth was measured weekly as previously described. Average sizes of the tumors ± 1 SE are shown; *D,* representative tumors at 5 weeks in animals inoculated with equivalent number of cells from each of the indicated cell lines.

Discussion

One of the central issues concerning c-Myc-regulated genes is the extent to which their functions are dependent upon the concurrent expression of other c-Myc targets, and thus upon c-Myc itself. This question arises as a consequence of most reported reconstitution studies having been conducted in cells which express c-Myc. Exceptions to this include studies with the target genes *Cul1*, *SHMT*, and *CDK4*, all of which can complement the growth deficit and/or cell cycle abnormality in KO cells to varying degrees (29, 31, 35). However, for the vast majority of c-Myc targets, the degree to which they require the proper regulation of other c-Myc target genes, or what these targets might be, remains unresolved. Moreover, because of their limited functional overlap with c-Myc, the genes which have been assessed in KO cells have been tested for only a limited number of c-Myc-like activities.

MT-MC1 enjoys an unusual status among c-Myc target genes in that it mimics a broad range of c-Myc phenotypes, some quite strongly (38). Although HMG-I has not been as extensively explored, its central role in transformation has been demonstrated by showing that its inhibition results in a severe impairment of c-Myc-mediated *in vitro* tumor cell growth and *in vivo* tumorigenesis. Furthermore, lymphoid-specific transgenic expression of HMG-I results in a high incidence of lymphoid malignancies (33, 49).

Given the substantial contributions of MT-MC1 and HMG-I to the c-Myc phenotype, we have explored the need for concurrent endogenous c-Myc expression in mediating their effects, as well as their cooperation with one another. Our results show that some, but not all, of the known c-Myc phenotypes can be recapitulated by both MT-MC1 and HMG-I in a c-Myc–independent manner. However, the overall nature of these changes, although overlapping, was distinct for the two genes. For example, MT-MC1 was qualitatively similar to c-Myc in restoring the normal morphology of KO cells, albeit somewhat less efficiently (Fig. 1*B*). In contrast, HMG-I, although being better at altering KO cell morphology, produced unique structural alterations. In combination, MTMC1 and HMG-I produced a heterogeneous population of both cell types whose individual morphologies may reflect the relative abundance of the two proteins.

The effects of MT-MC1 and HMG-I on KO growth rates were also quite distinct. Whereas the ability of HMG-I to accelerate KO cell proliferation was seen immediately, the effect of MT-MC1 was observed only after several weeks of *in vitro* culture. These findings suggest that, although both MT-MC1 and HMG-I function in a c-Myc–independent manner to accelerate proliferation, they do so via different pathways. The delayed action of MT-MC1 suggests that its mechanism is indirect, whereas HMG-I's immediate effect suggests that its mechanism is more akin to that of Cul1, CDK4, and SHMT, each of which can immediately complement the growth defect of KO cells, albeit to variable degrees (29, 31, 35).

The appearance of tetraploidy in KO-MT-MC1 cells also occurred with a delayed onset and paralleled the emergence of

A.

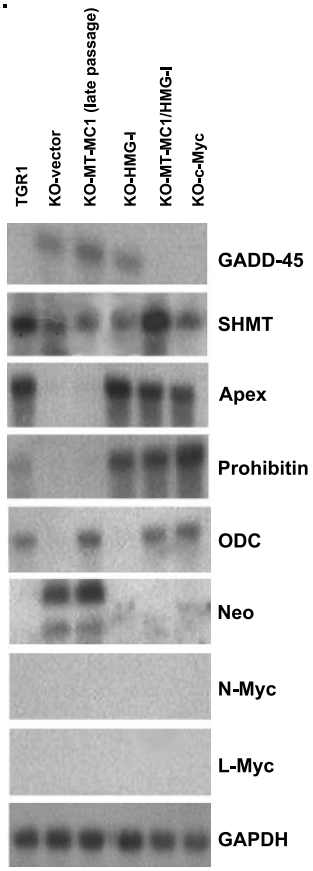

B.

Target Sequence	Expression Relative to TGR1				
	KO-vector	KO-MT-MC1	KO-HMG-I	KO-MT-MC1/HMG-I	KO-c-Myc
Nucleolin	***1.14*** ± .04	***1.27*** ± .03	***2.43*** ± 0.19	***2.10*** ± .01	***4.96*** ± .06
Transferrin Receptor	***0.32*** ± .03	***0.24*** ± .003	***3.29*** ± 0.36	***2.58*** ± 0.34	***1.72*** ± .04
Nopp 140	1.22 ± .05	0.94 ± 0.11	***3.39*** ± 0.15	***3.06*** ± .06	***3.67*** ± 0.10
Timp 2	***2.52*** ± 0.16	***2.33*** ± .09	0.62 ± .03	0.88 ± .02	0.92 ± .04
Tip 49	***0.38*** ± .00	0.32 ± .06	1.26 ± 0.17	1.26 ± .06	1.70 ± 0.11
Rcl	1.00 ± 0.19	1.00 ± 0.19	1.44 ± 0.11	1.33 ± .00	***3.11*** ± 0.29
Cyclin E	***1.46*** ± .08	1.07 ± 0.12	***5.72*** ± 0.52	***5.09*** ± 0.75	***3.09*** ± 0.55

Figure 6. Comparison of gene expression profiles. *A,* Northern analyses, 5 μg of total RNA from each of the indicated cell lines was used to generate Northern blots, which were then hybridized with coding region probes for the indicated genes (38). Note that a neomycin probe served as a surrogate marker for endogenous c-Myc regulation since a neo cassette was inserted into the c-Myc locus during the creation of the original KO cell line (50). As a control for RNA loading, one of the blots was stripped and hybridized with a glyceraldehyde-3-phosphate dehydrogenase probe. KO-MT-MC1 RNA was prepared from late passage, rapidly growing cells; *B,* quantitative real-time PCR analyses of select c-Myc target genes. Real-time PCR analyses were done using a Quantitect SYBR Green kit (Qiagen). The numbers represent the averages of triplicate determinations and are expressed relative to the levels of the indicated target transcript measured simultaneously in TGR1 cells. Significant differences ($P < 0.05$) relative to TGR1 levels are indicated in bold, italicized type.

the rapid growth phenotype and clonogenicity. This effect on karyotype mirrored the action of MT-MC1 in other cell types (38) as well as the action of c-Myc itself when it is deregulated (20, 22, 23). The proposed link between genomic instability and accelerated proliferation is supported by our finding that KO-MT-MC1/HMG-I cells, which show rapid growth from the onset, remained diploid throughout the course of the study and thus escaped the need to develop tetraploidy.

Additional properties that were differentially affected by MT-MC1 and HMG-I were cell size and transformation (Figs. 4 and 5). In the former case, MT-MC1's ability to promote cell growth was immediate and thus unrelated to its more indirect effects on proliferation and ploidy. HMG-I's effect on cell size was also immediate, although opposite that of MT-MC1's. The intermediate size of KO-MT-MC1/HMG-I cells indicates that the two proteins are co-dominant for this phenotype. These findings also suggest that c-Myc's ability to promote growth may be under negative control by other target genes. Taken together, these observations show that increases in cell size and transformation, as mediated by MT-MC1 and HMG-I, are not invariably linked and can in fact be uncoupled (18, 19, 27).

It should be emphasized that three of the phenotypes of KO-MT-MC1 cells (rapid growth, chromosomal instability, and transformation) are seen only after they are cultured for 10 to 12 weeks and that it is currently not clear how these phenotypes relate to one another. Standard transformation assays, such as those reported here, probably require a certain minimal cellular growth rate, which may not have been met by early passage MT-MC1 cells. The failure of clonogenic survival may thus be more reflective of the limitations of these assays than of intrinsic differences in the degree of cellular transformation. On the other hand, it is now appreciated that several features of c-Myc-mediated transformation, including transformation itself, are neither the direct nor immediate result of the oncoprotein's action. c-Myc overexpression is associated with ongoing chromosomal instability as well as other types of DNA damage and repair defects (55–57, 61). Furthermore, whereas transformation of established cells is a direct and early result of c-Myc overexpression, this is not the case in primary cells, either *in vitro* or *in vivo*. Thus, it is tempting to speculate that MT-MC1 may represent a component of a pathway through which c-Myc can exert such indirect and late effects.

Perhaps the most conspicuous c-Myc phenotype that could *not* be mimicked by MT-MC1 or HMG-I, either individually or in combination, was that of enhanced apoptosis following serum withdrawal (21). This is particularly notable given the prominence of this property in KO cells which have been reconstituted by c-Myc or other members of the Myc family (Fig. 2*A* and ref. 51). Given that MT-MC1 accelerates apoptosis in other c-Myc-replete cells as well as or even better than c-Myc itself (38), our findings strongly suggest that it must do so in cooperation with other, as yet unidentified, c-Myc target genes (besides HMG-I). This underscores the need to characterize additional direct c-Myc target genes which cooperate with MT-MC1 and HMG-I to reconstitute a more complete c-Myc phenotype in KO cells. Obvious candidates which bear testing

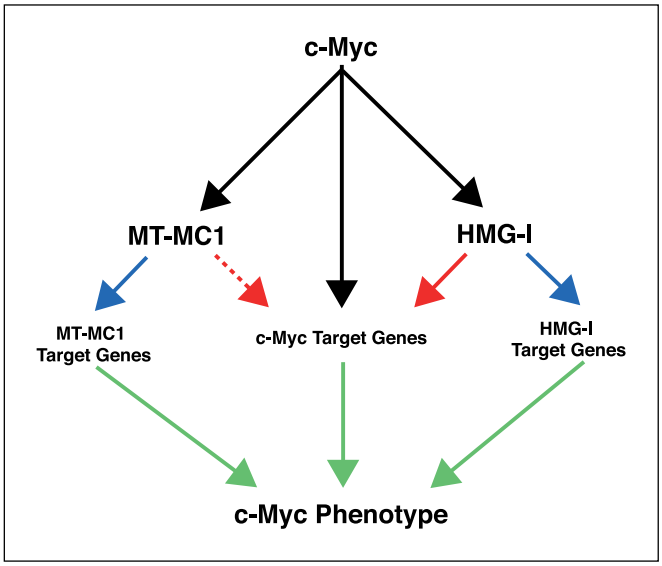

Figure 7. Model for c-Myc–dependent and independent phenotypic regulation by c-Myc target genes. c-Myc regulates a large number of genes, among which are its positive, direct targets MT-MC1 and HMG-I (*black arrows*). The latter two may regulate their own unique target genes (*blue arrows*) or other c-Myc targets (*red arrows*). Based on the results presented here, MT-MC1 may be a less efficient regulator of c-Myc target genes than HMG-I (*dashed red arrow*). Some phenotypes can be reconstituted by MT-MC1 or HMG-I alone, whereas others may require their cooperation and/or other c-Myc target genes (*green arrows*).

include those already known to impart a strongly proapoptotic response in c-Myc-expressing cells such as ornithine decarboxylase and Bax (28, 62). The cell lines described here should prove useful in evaluating the contributions of these additional genes.

Our limited Northern and quantitative real-time PCR analyses have indicated that overexpression of MT-MC1 and/or HMG-I can, in some cases, lead to the deregulation of other c-Myc target genes. These results suggest the existence of regulatory circuits in which certain genes are subject to control by c-Myc as well as the products of some of its direct targets, although not necessarily in an identical manner. The ability of HMG-I to promote chromatin remodeling (39–41) is certainly consistent with such a proposed role as are recent DNA microarray results indicating that some of the genes under the control of MT-MC1 and HMG-I consist of previously described c-Myc targets.[6,7] Somewhat surprising was the finding that a substantial fraction of the c-Myc target genes tested in the above assays were as responsive to HMG-I overexpression as they were to c-Myc (Fig. 6).

The results reported here suggest a model in which MT-MC1 and HMG-I each controls multiple and overlapping c-Myc–dependent and –independent phenotypes (Fig. 7). In the absence of c-Myc, the coordinated regulation of its other target genes is abrogated, although their unregulated expression may persist at some basal level (10, 53). If c-Myc–dependent control of these genes is crucial for a particular phenotype (for example the promotion of apoptosis), then it will not be recapitulated by the individual or combined expression of MT-MC1 or HMG-I. In contrast, if the control of these genes by c-Myc is not required for a phenotype, then it will be recapitulated by MT-MC1 and/or HMG-I. This model allows for the possibility that some phenotypes may be only partially reconstituted in the absence of c-Myc. It also allows for target genes to act additively as they to do in the case of transformation or the regulation of *gadd45* and *shmt* gene expression by the coexpression of MT-MC1 and HMG-1. It also provides for the products of genes such as MT-MC1 and HMG-I to circumvent c-Myc by acting as surrogate regulators of a subset of c-Myc target genes. This is clearly the case with HMG-I, which was unexpectedly found to regulate a significant subset of c-Myc targets in KO cells. The actual extent of this ability to substitute for c-Myc, and whether its apparent superiority to MT-MC1 in this regard holds true for other c-Myc targets remains to be determined.

In conclusion, we have shown that MT-MC1 and HMG-I can reconstitute multiple c-Myc phenotypes in a c-Myc–independent manner. These findings are consistent with the idea that, despite the myriad of targets under the control of c-Myc, only a small number are critical for achieving its most important properties. The success of this approach suggests that, through the selective investigation of other critical c-Myc targets, it will be possible to identify those which further restore the phenotype by, for example, promoting apoptosis. In this way, it seems possible that the entire c-Myc phenotype might be amenable to reconstitution by a defined set of target genes, although the nature of these, and the minimal number needed, may not be identical in all cases.

[6] K. Rogulski et al., manuscript in preparation.
[7] L.M.S. Resar, personal communication.

Acknowledgments

Received 8/12/2004; revised 11/11/2004; accepted 1/12/2005.

Grant support: NIH grants RO1 HL33741 and RO1 CA78259 to E.V. Prochownik.

The costs of publication of this article were defrayed in part by the payment of page charges. This article must therefore be hereby marked *advertisement* in accordance with 18 U.S.C. Section 1734 solely to indicate this fact.

We thank Linda Penn, Sarah Oster, and Garry Nolan for supplying retroviral reagents, packaging cell lines, and advice on cell sorting; Bob Lakomy for cell sorting; Linda Resar for helpful discussions; and Burhan Gharaibeh for karyotyping.

References

1. Nesbit CE, Tersak JM, Prochownik EV. MYC oncogenes and human neoplastic disease. Oncogene 1999; 18:3004–16.
2. Grandori C, Cowley SM, James LP, Eisenman RN. The Myc/Max/Mad network and the transcriptional control of cell behavior. Annu Rev Cell Dev Biol 2000;16:653–99.
3. Oster SK, Ho CS, Soucie EL, Penn LZ. The myc oncogene: MarvelouslY Complex. Adv Cancer Res 2002; 84:81–154.
4. Coller HA, Grandori C, Tamayo P, et al. Expression analysis with oligonucleotide microarrays reveals that MYC regulates genes involved in growth, cell cycle, signaling, and adhesion. Proc Natl Acad Sci U S A 2000;97:3260–5.
5. Guo QM, Malek RL, Kim S, et al. Identification of c-myc responsive genes using rat cDNA microarray. Cancer Res 2000;60:5922–8.
6. Nesbit CE, Tersak JM, Grove LE, Drzal A, Choi H, Prochownik EV. Genetic dissection of c-myc apoptotic pathways. Oncogene 2000;19:3200–12.
7. Neiman PE, Ruddell A, Jasoni C, et al. Analysis of gene expression during myc oncogene-induced lymphomagenesis in the bursa of Fabricius. Proc Natl Acad Sci U S A 2001;98:6378–83.
8. Schuhmacher M, Kohlhuber F, Holzel M, et al. The transcriptional program of a human B cell line in response to Myc. Nucleic Acids Res 2001; 29:397–406.
9. Fernandez PC, Frank SR, Wang L, et al. Genomic targets of the human c-Myc protein. Genes Dev 2003;17: 1115–29.
10. Levens DL. Reconstructing MYC. Genes Dev 2003; 17:1071–7.
11. O'Connell BC, Cheung AF, Simkevich CP, et al. A large scale genetic analysis of c-Myc-regulated gene expression patterns. J Biol Chem 2003;278:12563–73.
12. Orian A, van Steensel B, Delrow J, et al. Genomic binding by the *Drosophila* Myc, Max, Mad/Mnt transcription factor network. Genes Dev 2003;17: 1101–14.

13. Li Z, Van Calcar S, Qu C, Cavenee WK, Zhang MQ, Ren B. A global transcriptional regulatory role for c-Myc in Burkitt's lymphoma cells. Proc Natl Acad Sci U S A 2003;100:8164–6.
14. Coppola JA, Cole MD. Constitutive c-myc oncogene expression blocks mouse erythroleukaemia cell differentiation but not commitment. Nature 1986;320:760–3.
15. Prochownik EV, Kukowska J. Deregulated expression of c-myc by murine erythroleukaemia cells prevents differentiation. Nature 1986;322:848–50.
16. Stern DF, Roberts AB, Roche NS, Sporn MB, Weinberg RA. Differential responsiveness of myc- and ras-transfected cells to growth factors: selective stimulation of myc-transfected cells by epidermal growth factor. Mol Cell Biol 1986;6:870–7.
17. Prochownik EV, Kukowska J, Rodgers C. c-myc antisense transcripts accelerate differentiation and inhibit G_1 progression in murine erythroleukemia cells. Mol Cell Biol 1988;8:3683–95.
18. Iritani BM, Eisenman RN. c-Myc enhances protein synthesis and cell size during B lymphocyte development. Proc Natl Acad Sci U S A 1999;96:13180–4.
19. Johnston LA, Prober DA, Edgar BA, Eisenman RN, Gallant P. *Drosophila* myc regulates cellular growth during development. Cell 1999;98:779–90.
20. Li Q, Dang CV. c-Myc overexpression uncouples DNA replication from mitosis. Mol Cell Biol 1999;19:5339–51.
21. Prendergast GC. Mechanisms of apoptosis by c-Myc. Oncogene 1999;18:2967–87.
22. Yin XY, Grove L, Datta NS, Long MW, Prochownik EV. C-myc overexpression and p53 loss cooperate to promote genomic instability. Oncogene 1999;18:1177–84.
23. Yin XY, Grove L, Datta NS, Katula K, Long MW, Prochownik EV. Inverse regulation of cyclin B1 by c-Myc and p53 and induction of tetraploidy by cyclin B1 overexpression. Cancer Res 2001;61:6487–93.
24. Fest T, Mougey V, Dalstein V, et al. c-MYC overexpression in Ba/F3 cells simultaneously elicits genomic instability and apoptosis. Oncogene 2002;21:2981–90.
25. Obaya AJ, Kotenko I, Cole MD, Sedivy JM. The proto-oncogene c-myc acts through the cyclin-dependent kinase (Cdk) inhibitor p27(Kip1) to facilitate the activation of Cdk4/6 and early G(1) phase progression. J Biol Chem 2002;277:31263–9.
26. Schorl C, Sedivy JM. Loss of protooncogene c-Myc function impedes G_1 phase progression both before and after the restriction point. Mol Biol Cell 2003;4:823–35.
27. Maines JZ, Stevens LM, Tong X, Stein D. *Drosophila* dMyc is required for ovary cell growth and endoreplication. Development 2004;131:775–86.
28. Packham G, Cleveland JL. Ornithine decarboxylase is a mediator of c-Myc-induced apoptosis. Mol Cell Biol 1994;14:5741–7.
29. Hermeking H, Rago C, Schuhmacher M, et al. Identification of CDK4 as a target of c-MYC. Proc Natl Acad Sci U S A 2000;97:2229–34.
30. Lewis BC, Prescott JE, Campbell SE, Shim H, Orlowski RZ, Dang CV. Tumor induction by the c-Myc target genes rcl and lactate dehydrogenase A. Cancer Res 2000;60:6178–83.
31. O'Hagan RC, Ohh M, David G, et al. Myc-enhanced expression of Cul1 promotes ubiquitin-dependent proteolysis and cell cycle progression. Genes Dev 2000;4:2185–91.
32. Wood LJ, Maher JF, Bunton TE, Resar LM. The oncogenic properties of the HMG-I gene family. Cancer Res 2000;60:4256–61.
33. Wood LJ, Mukherjee M, Dolde CE, et al. HMG-I/Y, a new c-Myc target gene and potential oncogene. Mol Cell Biol 2000;20:5490–502.
34. Prescott JE, Osthus RC, Lee LA, et al. A novel c-Myc-responsive gene, JPO1, participates in neoplastic transformation. J Biol Chem 2001;276:48276–84.
35. Nikiforov MA, Chandriani S, O'Connell B, et al. A functional screen for Myc-responsive genes reveals serine hydroxymethyltransferase, a major source of the one-carbon unit for cell metabolism. Mol Cell Biol 2002;22:5793–800.
36. Wonsey DR, Zeller KI, Dang CV. The c-Myc target gene PRDX3 is required for mitochondrial homeostasis and neoplastic transformation. Proc Natl Acad Sci U S A 2002;99:6649–54.
37. Lewis BC, Shim H, Li Q, et al. Identification of putative c-Myc-responsive genes: characterization of rcl, a novel growth-related gene. Mol Cell Biol 1997;17:4967–78.
38. Yin X, Grove L, Rogulski K, Prochownik EV. Myc target in myeloid cells-1, a novel c-Myc target, recapitulates multiple c-Myc phenotypes. J Biol Chem 2002;277:19998–20010.
39. Johnson KR, Cook SA, Davisson MT. Localization of the murine gene and two related sequences encoding high-mobility-group I and Y proteins. Genomics 1992;12:503–9.
40. Friedmann M, Holth LT, Zoghbi HY, Reeves R. Organization, inducible-expression and chromosome localization of the human HMG-I(Y) nonhistone protein gene. Nucleic Acids Res 1993;21:4259–67.
41. Reeves R, Beckerbauer L. HMG-I/Y proteins: flexible regulators of transcription and chromatin structure. Biochim Biophys Acta 2001;1519:13–29.
42. Homurra F, Katabami M, Leaner VD, et al. HMG-I/Y is a c-Jun/activator protein-1 target gene and is necessary for c-Jun-induced anchorage-independent growth in Rat1a cells. Mol Cancer Res 2004;2:305–14.
43. Ram TG, Reeves R, Hosick HL. Elevated high mobility group-I(Y) gene expression is associated with progressive transformation of mouse mammary epithelial cells. Cancer Res 1993;53:2655–60.
44. Tamimi Y, van der Poel HG, Denyn MM, et al. Increased expression of high mobility group protein I(Y) in high grade prostatic cancer determined by *in situ* hybridization. Cancer Res 1993;5512–6.
45. Chiappetta G, Manfioletti G, Pentimalli F, et al. High mobility group HMGI(Y) protein expression in human colorectal hyperplastic and neoplastic diseases. Int J Cancer 2001;91:147–51.
46. Rajeswari MR, Singh D, Jain A, Ray R. Elevated levels of high-mobility-group chromosomal proteins, HMGA1, in murine skin carcinoma. Cancer Lett 2001;173:93–9.
47. Dolde CE, Mukherjee M, Cho C, Resar LM. HMG-I/Y in human breast cancer cell lines. Breast Cancer Res Treat 2002;71:181–9.
48. Leman ES, Madigan MC, Brunagel G, Takaha N, Coffey DS, Getzenberg RH. Nuclear matrix localization of high mobility group protein I(Y) in a transgenic mouse model for prostate cancer. J Cell Biochem 2003;88:599–608.
49. Xu Y, Sumter TF, Bhattacharya R, et al. The HMG-I oncogene causes highly penetrant, aggressive lymphoid malignancy in transgenic mice and is overexpressed in human leukemia. Cancer Res 2004;64:3371–5.
50. Mateyak MK, Obaya AJ, Adachi S, Sedivy JM. Phenotypes of c-Myc-deficient rat fibroblasts isolated by targeted homologous recombination. Cell Growth Differ 1997;8:1039–48.
51. Landay M, Oster SK, Khosravi F, et al. Promotion of growth and apoptosis in c-myc nullizygous fibroblasts by other members of the myc oncoprotein family. Cell Death Differ 2000;7:697–705.
52. de Alboran IM, O'Hagan RC, Gartner F, et al. Analysis of C-MYC function in normal cells via conditional gene-targeted mutation. Immunity 2001;14:45–55.
53. Bush A, Mateyak M, Dugan K, et al. c-myc null cells misregulate cad and gadd45 but not other proposed c-Myc targets. Genes Dev 1998;12:3797–802.
54. Small J, Rottner K, Hahne P, Anderson KI. Visualising the actin cytoskeleton. Microsc Res Tech 1999;47:3–17.
55. Vafa O, Wade M, Kern S, et al. c-Myc can induce DNA damage, increase reactive oxygen species, and mitigate p53 function: a mechanism for oncogene-induced genetic instability. Mol Cell 2002;9:1031–44.
56. Karlsson A, Deb-Basu D, Cherry A, Turner S, Ford J, Felsher DW. Defective double-strand DNA break repair and chromosomal translocations by MYC overexpression. Proc Natl Acad Sci U S A 2003;100:9974–9.
57. Karlsson A, Giuriato S, Tang F, Fung-Weier J, Levan G, Felsher DW. Genomically complex lymphomas undergo sustained tumor regression upon MYC inactivation unless they acquire novel chromosomal translocations. Blood 2003;101:2797–803.
58. Gomez-Roman N, Grandori C, Eisenman RN, White RJ. Direct activation of RNA polymerase III transcription by c-Myc. Nature 2003;421:290–4.
59. Marhin WW, Chen S, Facchini LM, Fornace AJ Jr, Penn LZ. Myc represses the growth arrest gene gadd45. Oncogene 1997;14:2825–34.
60. Luo Q, Li J, Cenkci B, Kretzner L. Autorepression of c-myc requires both initiator and E2F-binding site elements and cooperation with the p107 gene product. Oncogene 2004;23:1088–97.
61. Soucek L, Evan G. Myc—is this the oncogene from hell? Cancer Cell 2002;1:406–8.
62. Mitchell KO, Ricci MS, Miyashita T, et al. Bax is a transcriptional target and mediator of c-myc-induced apoptosis. Cancer Res 2000;60:6318–25.

C-Myc–Independent Restoration of Multiple Phenotypes by Two C-Myc Target Genes with Overlapping Functions

Krisiti Rothermund, Kenneth Rogulski, Elaine Fernandes, et al.

Cancer Res 2005;65:2097-2107.